

UDC 621.548

EVALUATION OF THE INFLUENCES OF DIFFERENT ROOF SHAPES ON THE FLOW PROPERTIES AND PERFORMANCE OF SMALL WIND TURBINES

Alexander Hirschl

hirschl@technikum-wien.at

ORCID: 0009-0009-8351-1415

Daniel Österreicher

daniel.oesterreicher@technikum-wien.at

University of Applied Sciences
Technikum Wien,
Höchstädtplatz 6, 1200 Wien, Austria

Small wind turbines offer a complement to photovoltaic systems and are becoming an interesting solution in the wake of rising energy prices. The measurement results indicate that some locations on and around the building are not suited for installing wind turbines, while others show increased wind potential. Due to limited space, rooftop mounting is an interesting alternative to free mounting on a mast from a technical point of view. For this reason, the influence of roof shapes on the flow on and behind the building was measured and the performance of two different types of small wind turbines was investigated. The turbines assessed in the project are VertikonM with a vertical axis and helix-shaped rotor blades, and Superwind 1250 wind turbine with a horizontal axis and centrifugal force pitch control. The results showed that there is an average increase in wind speed of 0.2 m/s on gable roofs at hub height (7 m). In comparison, there is an increase of 0.4 m/s on flat roofs at hub height (7 m). In relation to the performance of the turbines, high turbulence on the roof seems to cancel out this effect. The performance of the horizontal axis small wind turbine has not increased in comparison with gable roof and free-standing mast. For the vertical-axis turbine, a power increase by a factor of 2.23 was achieved between free-standing mast and gable roof. Vertical wind flow above the gable roof was identified as the main cause for power increase. The experiment was conducted on the Lichtenegg energy research park (Lower Austria) and its results make it possible to better identify all effects that affect the turbine output power.

Keywords: small wind turbine, building roof, wind speed, turbulence intensity, power.

Nomenclature

ρ_{1min}	air density [kg/m ³]	R_w	gas constant water vapour 461.5 [J/kgK]
T_{1min}	temperature [K]	p_w	vapour pressure $0.0000205 \cdot e^{0.631846 \cdot T_{1min}}$
B_{1min}	ambient air pressure [Pa]	V_n	normalised wind speed [m/s]
R_0	gas constant 287.05 [J/kgK]	ρ_0	reference air density [kg/m ³]
Φ	relative humidity [0 to 1]	V_{1min}	measured wind speed [m/s]

Introduction

Alongside photovoltaics, small wind turbines (SWT) are another feasible way to yield energy in an environmentally friendly way in populated areas. Currently, SWT have primarily been of interest to farmers and commercial enterprises and usually have been installed at a certain distance from buildings and obstacles aiming for an undisturbed laminar flow. However, the growing desire for private energy autonomy brought SWT in the focus of private households, developers, building and energy planners and architects [1]. Thus, decreasing the distance of SWT to populated areas or even leading to roof-top installations. These turbines are preferably installed in hub heights less than 30 m, exposing them, especially in the built environment to complex airflows, vortices and other aerodynamic effects. Common structures such as flat and gabled roofs feature complex flows. Currently, the common approach to assess the fluid mechanics of a SWT on or nearby a building is to perform CFD simulations. The main findings of the studies conducted so far have been simulations or model measurements in a wind tunnel, which cannot entirely display all effects on the power output of a turbine. Practical experiences and measurements which might verify or improve simulation are currently not available. The only study on this subject, which is based on measured values, is one of the Technical University of Denmark (DTU) confirming known effects such as the bubble separation behind buildings [2].

Aim of the work

In order to investigate the influence of different roof shapes on the performance of small wind turbines, two building models with a gabled and a flat roof were constructed in the Lichtenegg energy research park

This work is licensed under a Creative Commons Attribution 4.0 International License.

© Alexander Hirschl, Daniel Österreicher, 2023

(Lower Austria). The objective of the project was to examine two different roof mounted SWT technologies. A vertical-axis small wind turbine (VASWT) and a horizontal-axis small wind turbine (HASWT) were investigated under real life conditions, considering the influence of the roof shape. The main focus thereby was:

- An evaluation of the impact of complex obstacles (building with various roof shapes) on the local flow pattern as well as on the flow in turbine hub height under real conditions;
- A metrological evaluation of the influence of the roof shape on the performance of SWT.

Method

Firstly, the flow properties of the test field were investigated without buildings in order to create a site calibration. Afterwards, the flow patterns on and around two buildings (flat and gabled roof) were measured with ultra-sonic-anemometers installed on met masts, measuring horizontal and vertical wind speed as well as the wind direction. The sensors were positioned in 3.5 m, 7 m and 10.5 m in front of and behind the building as well as on the building in 7 and 10.5 m, enabling the investigation of vortices and turbulences. Only measurement values perpendicular to the gable of the building were investigated. The values were recorded with a sample rate of 1 Hz and were converted to 1-minute average, maximum, minimum and standard deviation values. The reference to the wind speed above the building was the met mast in front of the building, which was exposed to the free stream without any obstacle induced disturbance.

Secondly, two types of SWT were installed on the buildings in a hub height of 7 m. In order to compare whether a roof shape is advantageous to the energy yield or not, each turbine was investigated on the flat roof, gabled roof and a standalone mast. The power output was measured with the same sample rate as the meteorological data. Power curves were calculated according to the current standard IEC 61400-12 [3] levelling the values to a reference air density of 1,225 kg/m³ to ensure comparability.

Infrastructure

The building models and SWT were placed on the ridge of a hill at 800 m above sea level in the "Lichtenegg energy research park", featuring an annual average wind speed of 5.1 m/s. The pre-evaluation of the main wind direction was crucial for the position of the buildings investigated because only an inflow perpendicular to the roof ridge was of interest within the project. Previous measurements of the main wind direction revealed two main wind sectors in 315° with a frequency of occurrence of 23% and 180° occurring with a frequency of 21%. The terrain on which the buildings were installed is sloping downwards with an angle of 7°, representing an uneven and complex surface in terms of fluid dynamics.

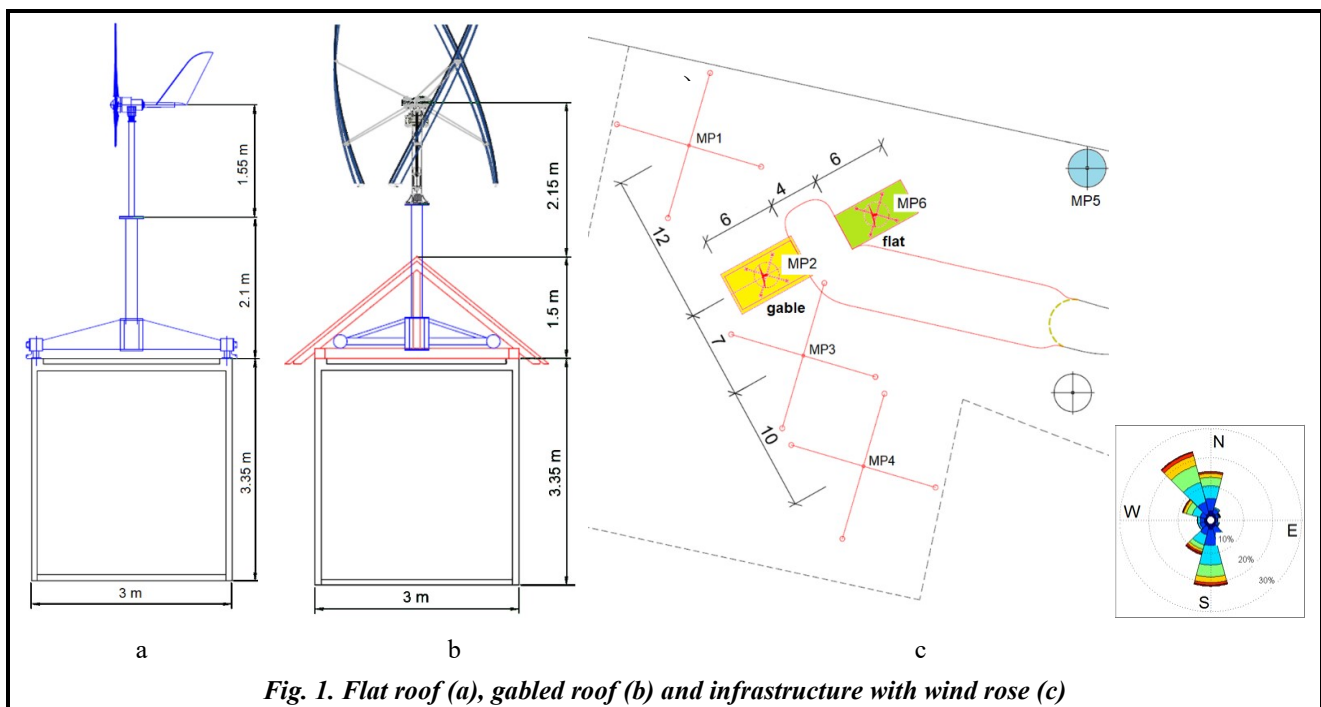


Fig. 1. Flat roof (a), gabled roof (b) and infrastructure with wind rose (c)

Buildings

Studies with wind tunnel tests have shown that different roof shapes lead to a modified flow pattern [4] having the potential to influence the performance of a roof-top installed small wind turbine. For this reason, two typical roof shapes, gabled and flat roof were evaluated during the tests. The two buildings were realized as precast concrete garages to reproduce a typical application scenario for a building mounted small wind turbine. For further evaluation of the impact of the buildings on small wind turbines and human beings, it was important to choose a garage made of concrete to have to have similar propagation characteristics for structure borne noise and oscillations as in residential buildings. In this test setup, those buildings were smaller than real private housing due to space limitations on the test site. With dimensions of 6 m in length, 3 m in width and 3.35 m in height, the buildings represent the size of a small garage. Fig. 1, a–b show the vertical section of the flat roof with a height of 3.35 m and the gabled roof with a total height of 4.85 m. Each mast installation on the building results in a total hub height of the SWT of 7 m allowing comparable settings. Due to the frequency of occurrence of winds coming from 315° (see wind rose Fig. 1, c), the roof ridge of the buildings was aligned perpendicular to this sector. Before the installation of the small wind turbines, a met mast was installed on the buildings in order to understand the flow characteristics above the roof in hub height.

Wind measurement

Fig. 2 shows the measurement points MP1 to MP4 which are in line with the main wind direction 315°. The first mast (MP1) is installed in a distance of 10 m from the building centre, measuring the incident flow pattern. Before the measurement on the buildings, a site calibration was carried out without the buildings (see Fig. 2 violet sensor). To evaluate the impact of altered flow patterns impacting the SWT, the wind conditions at turbine hub height above the flat and gabled roof building were measured at MP2 in 7 m. The range of different effects of the roof on the boundary layer was measured with the sensor in 10.5 m at MP2.

Flow effects close to the roof were measured at MP2 in 5 m above ground on the flat roof (see Fig. 2 green sensor) and in 6 m above ground on the gabled roof (see Fig. 2 red sensor).

The flow pattern and wake effects behind the building were captured in 7 m distance from the building centre at MP3 and in 17 m distance from the building centre at MP4. On each mast, three 3D ultrasonic anemometers were installed at a height of 3.5 m, 7 m and 10.5 m (except MP3) above the ground (see Fig. 2).

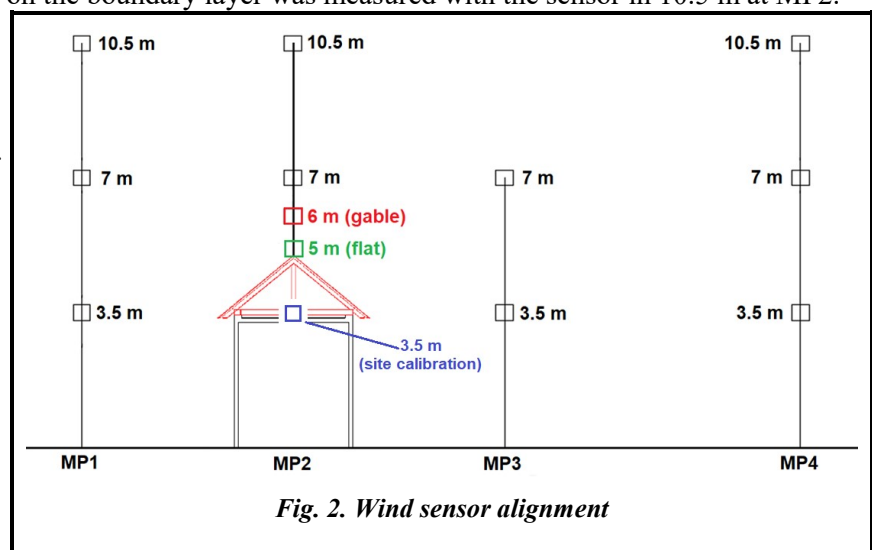


Fig. 2. Wind sensor alignment

All values were measured with a sample rate of 1 Hz in the data logger Ammonit Meteo 40 M. Those were subsequently evaluated as 1-minute average, maximum, minimum and standard deviation. The measurement of temperature, humidity and ambient pressure, which is essential for creating a standardized power curve, were recorded in the same time interval at measurement point MP1 in 5 m above the ground.

Small wind turbines and power measurement

The turbines assessed in the project were two different types according to the position of their rotation axis and type of rotor (Fig. 3). VertikonM represents a vertical axis small wind turbine with helix-shaped rotor blades, allowing the turbine to use vertical wind and horizontal wind. The turbines rated power is 0.95 kW and the dimensions of the carbon fibre reinforced glass fibre rotor is 2.4×2.48 m. The Superwind 1250 wind turbine is a horizontal axis small wind turbine with centrifugal force pitch control. Its rated power is 1.25 kW at a nominal wind speed of 11 m/s and the rotor blades are made of glass fibre, which is reinforced with carbon fibre.

Measurement point 2 (see Fig. 2) was replaced with the turbines in hub height at 7 m. The power output was measured with a power converter between the inverter and the grid connection terminal, emitting

an analogue electrical current signal which was recorded with the data logger sampling it with 1 Hz. Analogous to the meteorological values, the power was subsequently averaged for one minute and the maximum, minimum and standard deviation was calculated.

Power data of different time ranges feature altering temperature, humidity and ambient pressure values, directly affecting the energetic content of an air flow and the comparability of power curves. Thus, the power

evaluation is based on the IEC EN 61400-12. Firstly, the current ambient air density was calculated based on the standard specification according to formula (1).

$$\rho_{1 \min} = \frac{1}{T_{1 \min}} \cdot \left(\frac{B_{1 \min}}{R_0} - \Phi \cdot P_w \left(\frac{1}{R_0} - \frac{1}{R_w} \right) \right) \quad (1)$$

Secondly, measured data was standardized to the reference air density 1.225 kg/m³ at standard atmosphere (1013 hPa; 15 °C) according to formula (2) for turbines with pitch-control (Superwind 1250) or formula (3) for stall-control (VertikonM).

$$V_n = V_{1 \min} \left(\frac{\rho_{1 \min}}{\rho_0} \right)^{\frac{1}{3}}; \quad (2)$$

$$P_n = P_{1 \min} \left(\frac{\rho_{1 \min}}{\rho_0} \right). \quad (3)$$

Power values were classified in centred wind speed BINs with an increment of 0.5 m/s. The values in each BIN were averaged and if one BIN showed a number of data less than 10, this BIN was linearly interpolated [3]. Due to the measurement setup and the infrastructure, the evaluation of the power curves was not fully in line with the standard [3].

Flow pattern – flat & gabled roof

In order to draw conclusion, whether different roof shapes have a positive or negative influence on a roof installed small wind turbines power output, the influence of the roof on the incident flow was analysed based on the measured data. For this purpose, only measured values of the wind direction 315° (including values ±20° of main direction) were used allowing the analysis of wake effects behind the buildings with the values of the measurement point MP4. In order to exclude flow patterns of the terrain, the measured values of MP2 and MP4 with buildings were compared with the values without buildings (site calibration). The classification of the values was done with the BIN-procedure described in the IEC 61400-12 standard and in an increment of 0.5 m/s. Only values of the corresponding height and measurement point were compared, e.g. values from MP2 7 m flat roof were compared with MP2 7 m values from the site calibration. Additionally, the angle of vertical winds was evaluated for MP2 and MP4.

Fig. 4 shows the variance of the wind speed at MP2 for the gabled roof (a) and flat roof (b) in 10.5 m, 7 m. Close to the roof, the height of the third measurement point deviates to 6 m for the gabled and 5 m for flat roof. The wind speed progression at MP2 in Fig. 4, a, which refers to the gabled roof, indicates no increase of the wind speed in 10.5 m height in comparison to the free field (site calibration). This indicates that an obstacles influence on the boundary layers is less than 0.1 m/s in its double height, as also seen in CFD-simulations [5]. In 7 m (hub height) there is a slight increase of the wind speed of +0.2 m/s or +4% on average. Those findings are not in line with the results from Abohela et al. [6] who state that the wind speed above a gabled roof increases by +9.5%, according to CFD-simulations. The hub height in the simulations is 1.3 times higher than the building height. The differences between real measurement and simulation of Abohela et al. might come from the hub height difference, which is 7 m under real conditions and 6.3 m in



Fig. 3. VertikonM on gabled roof, Superwind 1250 on flat roof

the simulation. In contrast, in 6 m (1.15 m above the roofs gable) the wind speed increases from 10 m/s to 12 m/s in comparison to the free field, which is +20% and far above the simulation results.

The flat roof in Fig. 4, b, on the other hand, shows an even higher increase of the wind speed. The increase of the flat roof on the upper boundary layer in 10.5 m is ranging between +0.2 and +0.4 m/s in a wind speed range of 5 m/s and 10 m/s. The increase in 7 m height is even higher ranging +0.4 m/s and +0.9 m/s in the same wind speed range. On average the wind speed in hub height (7 m) increases by +9.5% which is far above the simulations results from Abohela et al. who calculated an increase of 7.5% in 4.3 m. In 5 m above the ground, 1.65 m above the flat roof respectively, the increase is up to +2 m/s. Hence, both roof shapes show an increase of the wind speed in each height, but the flat roof has the highest increase. This is probably due to a greater congestion in front of the building, resulting in an enhanced venturi effect above the building in hub height. It is also shown that real measurements deviate from simulations.

Fig. 5 refers to the wake effects 17 m behind the centre of the buildings. In Fig. 5, a, the effect of the gabled roof behind the building in stream wise direction is shown in the heights 10.5 m, 7 m and 3.5 m. It appears that in 10.5 m there is no influence noticeable, which indicates that an obstacle such as a gabled roof building has a local sphere of action in the wake of less than the double height of the obstacle. Contrary to that, the average wind speed in 7 m is diminished by -0.8m/s to -2 m/s in a wind speed range of 5 m/s to 10 m/s.

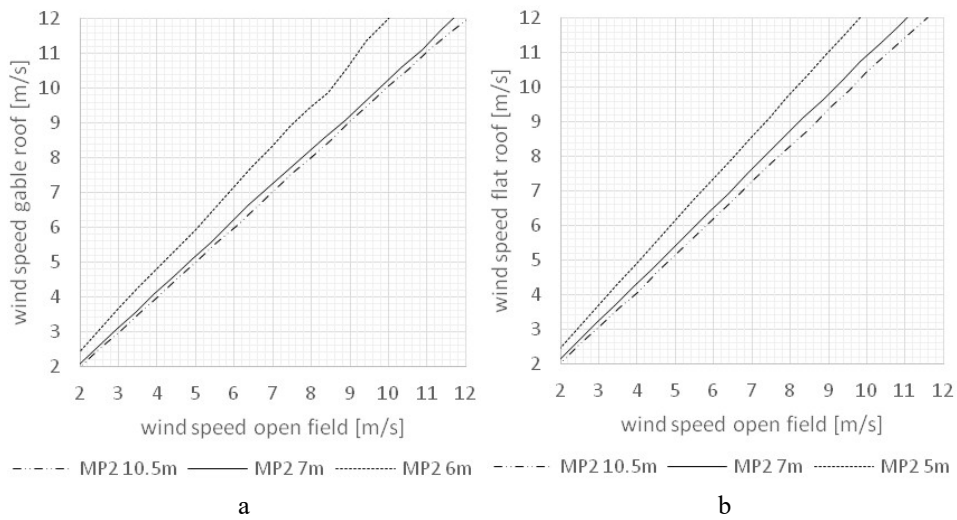


Fig. 4. Wind speed MP2 above gable(a) and flat(b) roof in reference to open field (site calibration)

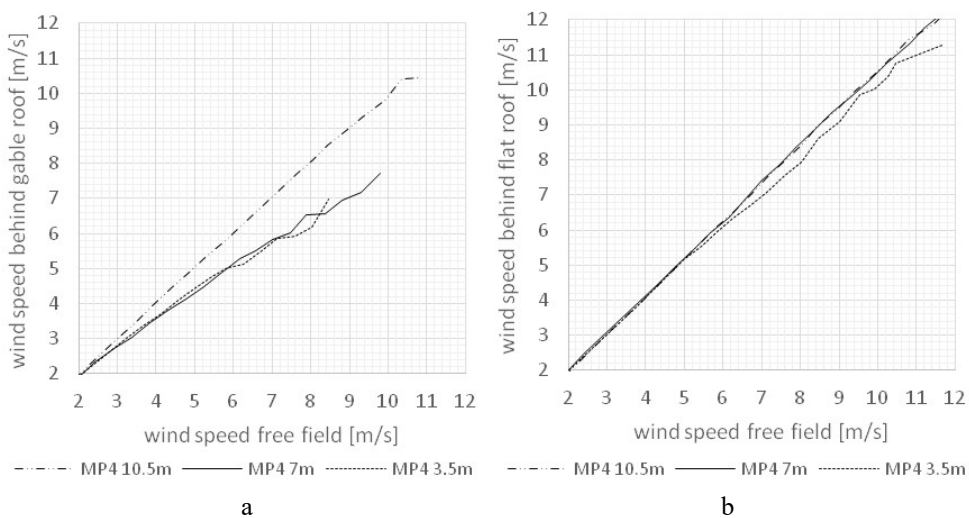


Fig. 5. Wind speed MP4 behind gable(a) and flat(b) roof in reference to free field (site calibration)

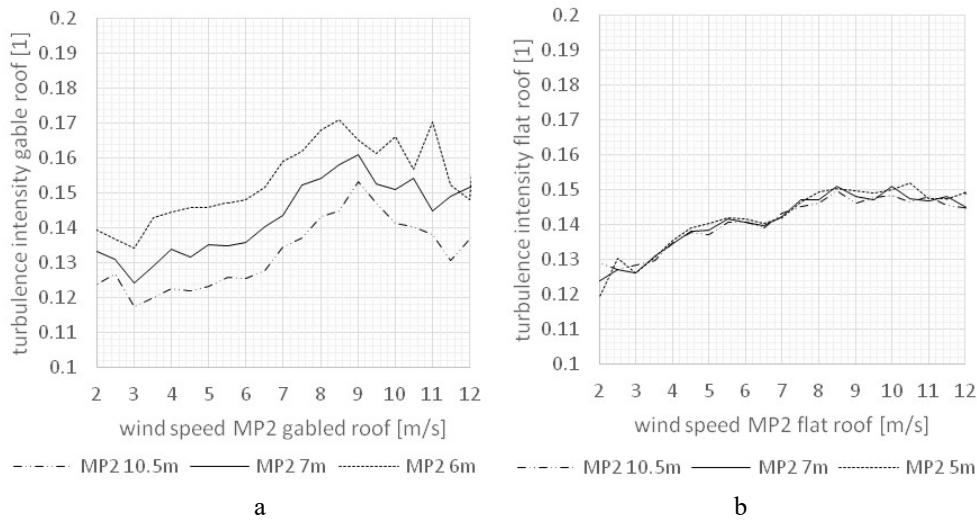


Fig. 6. Turbulence intensity MP2 above gable(a) and flat(b) roof in reference to wind speed

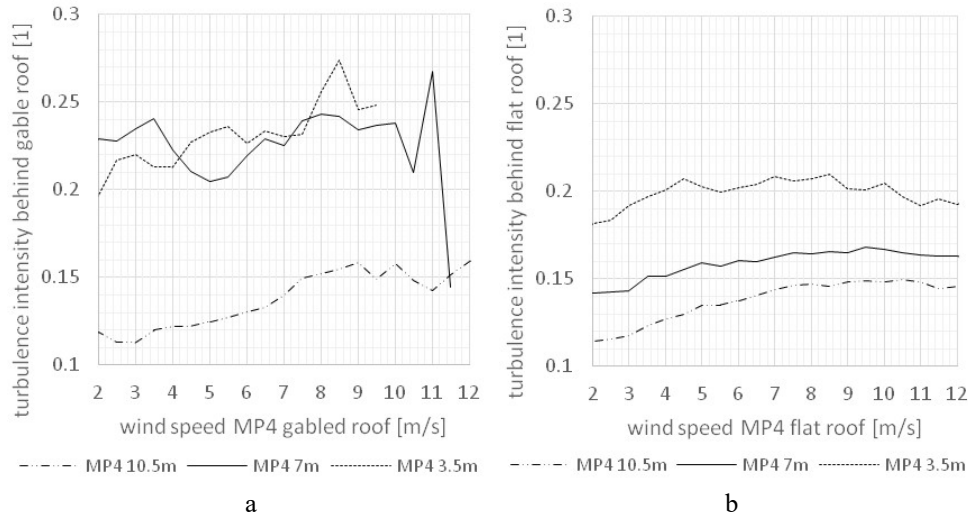


Fig. 7. Turbulence intensity MP4 above gable(a) and flat(b) roof in reference to wind speed

A similar progression is noticeable in 3.5 m height behind the gabled roof. According to simulations of Ledo et al. [5], a turbulent bubble forms behind the building with an expansion that does not significantly exceed the height of the gable. In addition, the wind speed profile far behind the building in the turbulent bubble can be described as relatively homogeneous in height and wind speed, as the dashed line (3.5 m) and continuous line (7 m) in Fig. 5, a are congruent.

Compared to the gabled roof, the flow in the vicinity of the flat roof has a much more undisturbed wind profile. In 10.5 and 7 m, a slight acceleration of +0.2 to +0.5 m/s is shown, which refers to an influence of the venturi effect above the flat roof. No acceleration effect can be measured at a height of 3.5 m. The much flatter extension of the turbulent bubble behind the flat roof is also confirmed in the CFD simulation results of Abohela et al.

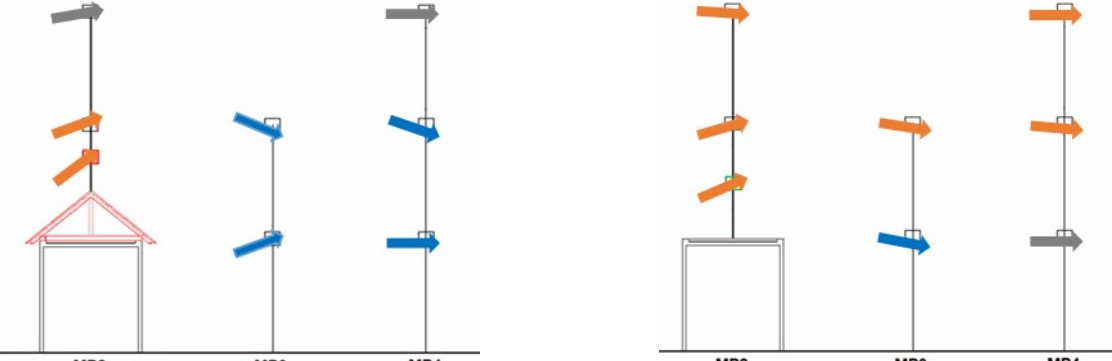
The turbulence intensity above the buildings at MP2 is shown in Fig. 6, a–b and shows different characteristics for each building shape. Above the gabled roof (see Fig. 6, a), the turbulence intensity fluctuates depending on the height and the current wind speed. Generally, it can be seen that a higher distance above the building leads to a lower turbulence intensity. In 10.5 m above the ground (5.65 m above the gabled roof) the turbulence intensity varies between 0.12 and 0.15, whereas in 7 m above the ground (2.15 m above the building) the range increased for 0.01 on average. The highest average values are measured in 6 m (1.15 m above the gable) ranging between 0.14 and 0.17. In contrast, the measurement points at MP2 above the flat roof

(Fig. 6, b) do not show any similarities to the gabled roof. In 10.5 m, 7 m and 5 m above the ground, the turbulence intensities have an almost congruent progression in a wind speed range of 2 to 12 m/s. In this case, the turbulence intensity increases constantly starting at 0.12/0.13 and reaching its maximum by 0.15. Anyway, the difference between the average turbulence intensities on both roof shapes can be classified as low.

In 17 m behind the building centre the turbulence intensity increases due to wake effects and vortices caused by the buildings itself. Fig. 7, a for instance, shows the turbulence intensity at MP4 for the gabled roof. In 10.5 m at MP4, there is no significant difference to MP2 at 10.5 m (see Fig. 6, a dashed line) noticeable, but in 7 m there is an increase of the turbulence intensity ranging between 0.2 and 0.25 with a substantial drop at 5 m/s, which is probably caused by a change of vortex separations. In Fig. 7, b, the progression of the turbulence intensity at MP4 behind the flat roof is rather homogenous with a lower turbulence intensity in all heights. The turbulence intensity in 10.5 is similar to the measured values at MP2 for the flat roof (see Fig. 6, b). In 7 m the turbulence intensity is slightly increased ranging between 0.14 and 0.17. Vortices caused by the building show a smaller extension in height and length than behind the gabled roof building, indicated by low turbulence values in 10.5 m and 7 m.

In order to compare the two building set-ups, the geometrical average value for the wind speed and turbulence intensity at every measurement point was calculated, limited to a wind speed range of 1 m/s to 10 m/s due to poor data quality above 10 m/s. The average angle of vertical wind was calculated as an arithmetical average for the same wind speed range. Table 1 shows the averaged values for the wind speed, turbulence intensity and angle of vertical wind. Additionally, the values are visualized with arrows on schemes of the measurement set up. Orange arrows indicate an increase of the wind speed, grey arrows – no increase and blue arrows – a decrease. Meanwhile, the angles of the arrows show the angle of vertical wind.

Table 1. In-/decrease of wind speed, turbulence intensity, angle of vertical wind above gabled and flat roof



Height	Measured values in the point			Height	Measured values in the point		
	MP2	MP3	MP4		MP2	MP3	MP4
10.5 m	+0.0 m/s 13% +1°	–	+0.0 m/s 13%	10.5 m	+0.2 m/s 14% -0.2°	–	+0.1 m/s 13%
7 m	+0.2 m/s 14% +5.4	-0.4 m/s 24% -5.8°	-0.6 m/s 23% -4.8°	7 m	+0.4 m/s 14% +1.8°	+0.5 m/s 14% -5.0°	+0.2 m/s 16% -4.5°
6/ 3.5 m	+0.9 m/s 15% +11.7	-3.0 m/s 53% +2.2°	-0.7 m/s 22%	5/ 3.5 m	+1.1 m/s 14% +3.2°	-2.1 m/s 44% -4.3°	+0.0 m/s 20%

SWT power – flat & gabled roof

The power output of the turbines was measured on the flat and gabled roof as well as on a standalone mast to enable comparability. The referenced wind direction was in all cases 315° with a deviation of ±20°. Due to the change of air density influencing the specific energy of wind, the wind speed or output power (depending on the type of turbine) was standardized according to formula (2) and (3). The power values were assigned to their corresponding BINs, according to the BIN-method in the IEC 61400-12 standard.

Fig. 8 shows the power curves measured on the flat roof (green line), gabled roof (red line) and on the standalone mast (black line) for the vertical axis Darrieus helix rotor VASWT VertikonM (see Fig. 1, a).

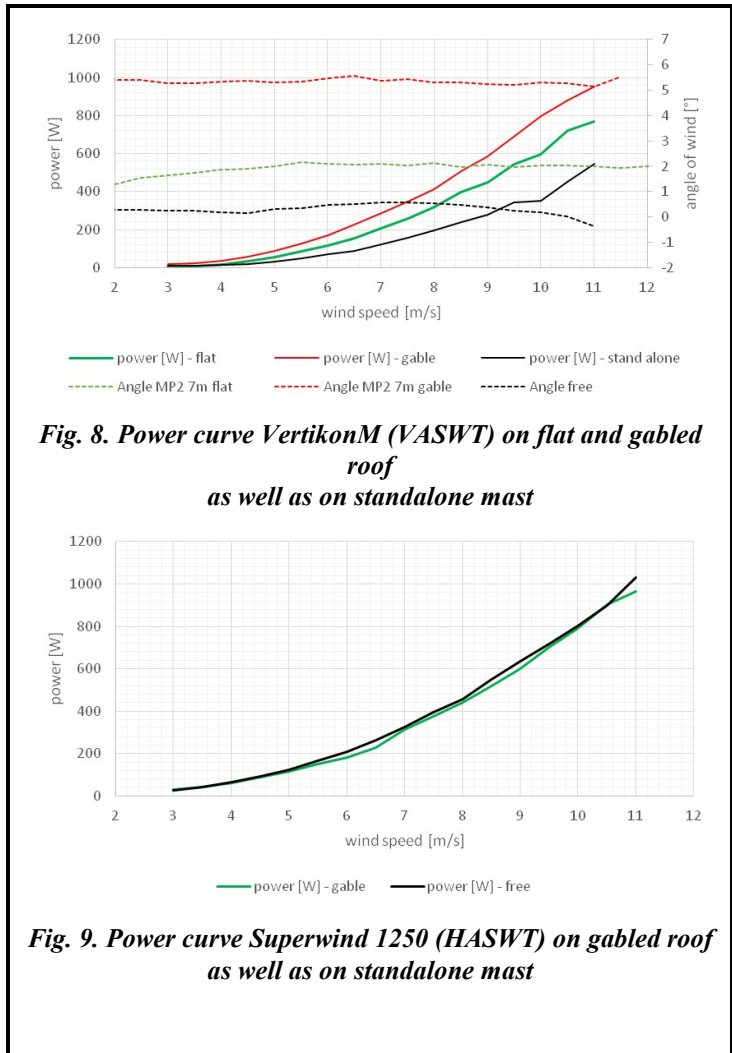
It can be seen that between the power curves of the gable roof and flat roof, the power values are 50 to 400 W higher. Compared to the stand-alone mast, the average power increase on the gable roof is a factor of 2.23. On the flat roof, the average power increase is a factor of 1.38. Although the average wind speed is greater on the flat roof than on the gable roof, the average power on the gable roof is higher. The reason for this is the angle of the incident wind flow and the design of the small wind turbine. Vertical axis small wind turbines with helix shape can utilize vertical wind flows more efficiently. The angle of the wind flow on the gable roof (red dotted line) is on average 5.4°, on the flat roof 1.8° (green dotted line) and on the stand-alone mast 0° (black dotted line). This clearly shows a correlation between output power increase on a building and vertical wind flow angle.

Contrary to the VASWT the horizontal axis small wind turbine Superwind 1250 did not show a significant power increase on a roof. Due to a measurement failure on the flat roof, Fig. 9 only shows results from the gabled roof and stand-alone mast. It can be seen that the difference in power varies between 0 and 25 W. The horizontal axis wind turbine does not react to the wind speed increase on the gable roof of +0.2 m/s on average. The vertical wind flow on the gable roof does not seem to have an impact on the power output either.

Conclusions

The measurement results indicate that some locations on and around the building are not suited for installing wind turbines, while others show increased wind potential compared to an undisturbed boundary layer. The gabled roof showed an increase of the horizontal wind speed of +4 % in 7 m (2.15 m above the gable) which increases the wind energy potential [W/m²] by 12%. The reason for the increase is the congestion of the boundary layers, which causes an acceleration above the gable. Additionally, the pitched roof causes an average angle of 5.4° of the incident wind flow. The shape of the gabled roof building has shown effect in a height 1.44 times higher than the building. Eddies and vortices extend up to 17 m behind the building, which is more than 3.5 times the building height. In this zone highly turbulent vortices appeared showing turbulence intensities above 50%. Contrary to the highly turbulent zones behind the gabled roof, the flat roof showed a rather homogenous flow pattern. The wind speed above the flat roof in 7 m increased by 8% (3.65 m above the roof) on average, which leads to an increase of the specific wind potential [W/m²] by 25%. The missing pitched roof on the flat roof probably reduces the angle of vertical winds to +1.8° on average in 7 m and at the same time limits the extension of the turbulent flow in height and length. The turbulent flow behind the building appears to have an expansion of 3.5 m, which is 1.04 times the building height. A positive acceleration effect in 7 m height was still measurable in 17 m behind the building, which is 5 times the building height.

The power output of two different small wind turbines investigated on the roofs was not in line with the increase of the wind speed. Apparently, the gabled roof showed a higher impact on the power output than the flat roof, despite showing a lower wind speed increase. The main reason for higher power output appeared to be the vertical angle of the incident wind flow instead of increased wind speed.



References

1. Leeb, K. (2015). *Potenzial kleinwindkraft in Österreich* [Potential small wind power in Austria]. *Proceedings of the 1 Internationale Kleinwindtagung – Proceedings of the 1 International Small Wind Conference*, Austria, Vienna, 16 April 2015. Austria, Vienna: FH Technikum Wien, pp. 4–8 (in German).
2. Peña, A., Bechmann, A., Conti, D., Angelou, N., Mikkelsen, T., & Friis, P. (2015). Should we really be concerned about obstacles in wind resource assessment: Conference presentation. EWEA – Europe's Premier Wind Energy Event, France, Paris, November 17–20 2015. France, Paris: European Wind Energy Association. <http://www.ewea.org/annual2015/conference/allposters/PO142.pdf>.
3. (2017). Wind turbines. Part 12-1: Power performance measurements of electricity producing wind turbines IEC 61400-12-1: International Standard. International Electrotechnical Commission, 317 p.
4. Tominaga, Y., Akabayashi, S. I., Kitahara, T., & Arinami, Y. (2015). Air flow around isolated gable-roof buildings with different roof pitches: Wind tunnel experiments and CFD simulations. *Building and Environment*, vol. 84, pp. 204–213. <https://doi.org/10.1016/j.buildenv.2014.11.012>.
5. Ledo, L., Kosasih, P. B., & Cooper, P. (2011). Roof mounting site analysis for micro-wind turbines. *Renewable energy*, vol. 36, iss. 5, pp. 1379–1391. <https://doi.org/10.1016/j.renene.2010.10.030>.
6. Abohela, I., Hamza, N., & Dudek, S. (2013). Effect of roof shape, wind direction, building height and urban configuration on the energy yield and positioning of roof mounted wind turbines. *Renewable energy*, vol. 50, pp. 1106–1118. <https://doi.org/10.1016/j.renene.2012.08.068>.

Received 12 April 2023

Оцінка впливу різних форм дахів на властивості потоку та ефективність малих вітрових турбін

Alexander Hirschl, Daniel Österreicher

Університет прикладних наук Technikum Wien, Höchstädtplatz 6, 1200 Відень, Австрія

Малі вітрові турбіни можуть бути доповненням до фотоелектричних систем і викликати інтерес у зв'язку зі зростанням цін на енергію. Результати вимірювань показують, що деякі місця на будівлі та навколо неї не підходять для встановлення вітрових турбін, тоді як в інших спостерігається підвищений потенціал вітру. З технічної точки зору, через обмежений простір монтаж на даху є цікавою альтернативою вільному монтажу на щоглі. З цієї причини було виміряно вплив форми даху на потік на будівлі та за нею, а також досліджено ефективність двох різних типів невеликих вітрових турбін. У проєкті оцінювали турбіни VertikonM з вертикальною віссю та гвинтоподібними робочими лопатками та вітряну турбіну Superwind 1250 з горизонтальною віссю та керуванням кроком відцентрової сили. Результати показали, що на двохсхилих дахах на висоті втулки (7 м) спостерігається збільшення швидкості вітру в середньому на 0,2 м/с. Для порівняння, на плоских дахах на висоті втулки (7 м) спостерігається збільшення на 0,4 м/с. Що стосується ефективності турбін, то висока турбулентність на даху ніби нівелює цей ефект. Ефективність малої вітрової турбіни з горизонтальною віссю не збільшилася порівняно з двохсхилим дахом і окремою щоглою. Для турбіни з вертикальною віссю між окремою щоглою та двохсхилим дахом було досягнуто зростання потужності в 2,23 рази. Основною причиною збільшення потужності є вертикальний потік вітру над двохсхилим дахом. Експеримент проводився в енергетичному дослідницькому парку Lichtenegg (Нижня Австрія), і його результати дозволяють краще визначити всі ефекти, які впливають на вихідну потужність турбіни.

Ключові слова: мала вітрова турбіна, дах будівлі, швидкість вітру, інтенсивність турбулентності, потужність.

Література

1. Leeb K. Potential small wind power in Austria. *Proceedings of the 1 Internationale Kleinwindtagung*, Austria, Vienna, 16 April 2015. Austria, Vienna: FH Technikum Wien, 2015. P. 4–8.
2. Peña A., Bechmann A., Conti D., Angelou N., Mikkelsen T., Friis P. Should we really be concerned about obstacles in wind resource assessment: Conference presentation. EWEA – Europe's Premier Wind Energy Event, France, Paris, November 17–20 2015. France, Paris: European Wind Energy Association, 2015. <http://www.ewea.org/annual2015/conference/allposters/PO142.pdf>.
3. Wind turbines. Part 12-1: Power performance measurements of electricity producing wind turbines IEC 61400-12-1: International Standard. International Electrotechnical Commission, 2017. 317 p.

4. Tominaga Y., Akabayashi S. I., Kitahara T., Arinami Y. Air flow around isolated gable-roof buildings with different roof pitches: Wind tunnel experiments and CFD simulations. *Building and Environment*. 2015. Vol. 84. P. 204–213. <https://doi.org/10.1016/j.buildenv.2014.11.012>.
5. Ledo L., Kosasih P. B., Cooper P. Roof mounting site analysis for micro-wind turbines. *Renewable energy*. 2011. Vol. 36. Iss. 5. P. 1379–1391. <https://doi.org/10.1016/j.renene.2010.10.030>.
6. Abohela I., Hamza N., Dudek S. Effect of roof shape, wind direction, building height and urban configuration on the energy yield and positioning of roof mounted wind turbines. *Renewable energy*. 2013. Vol. 50. P. 1106–1118. <https://doi.org/10.1016/j.renene.2012.08.068>.

DOI: <https://doi.org/10.15407/pmach2023.01.033>

UDC 537.612; 543.3

EFFECT OF MAGNETIC FIELD ON OPTICAL DENSITY OF DISTILLED WATER

Volodymyr H. Mykhailenko

port342017@gmail.com

ORCID: 0000-0003-3082-6148

Yevhen F. Lukianov

ORCID: 0000-0001-8839-091X

Olha I. Lukianova

ORCID: 0000-0001-7235-7293

Tamara S. Vitkovska

ORCID: 0000-0001-6890-0441

Oleksandr Ye. Khinievich

ORCID: 0000-0003-1902-534X

Anatolii Pidhornyi Institute of Mechanical Engineering Problems of NAS of Ukraine, 2/10, Pozharskyi str., Kharkiv, 61046, Ukraine

Water is considered as the working fluid of wet steam turbine units. The importance of a purposeful change in the thermophysical properties of water used for energy needs is indicated. A reagent-free method (transverse magnetic field of permanent magnets) of influence on water is proposed. Literature data on currently available papers dedicated to the study of water properties is presented. It is shown that the mechanisms of influence of external physical fields on the physicochemical and thermophysical properties of water have not been elucidated as of now. It is emphasized that the properties of distilled water during exposure and after exposure to physical fields are even less studied. The currently existing contradictions between theoretical ideas about the properties of water and experimental results are considered. It was found that currently there are no correct methods and equipment capable of indicating changes in water properties in real time. As a solution, the equipment and method of analyzing the optical density of distilled water is proposed. The shortcomings of most existing experimental works on the study of the influence of physical fields on the optical density of water are analyzed. The requirements for devices intended for measuring the optical density of distilled water are formulated. A stand was made and experimental work on the study of the dependence of the optical density of distilled water on the induction of a magnetic field that affects it was carried out. It is proved that the magnetic field affects the optical density of distilled water in the infrared range of wavelengths both in the direction of increase (4.1%) and in the direction of decrease (1.7%) depending on the induction of the magnetic field and the speed of water flow through the working section of magnetization device. A hypothesis explaining the obtained result is proposed.

Keywords: magnetic field, optical density, magnetic field induction, distilled water.

Introduction

Water is the working fluid of wet steam turbine units. Its properties largely determine the design of the steam turbine and other elements of the wet steam turbine units to achieve maximum efficiency. The working body of the wet steam turbine unit in the liquid phase should have the lowest possible heat capacity, which brings the isobars in the T, S diagram as close as possible to the vertical, and its critical parameters to the maximum possible values. In this case, the thermal efficiency of the Rankine cycle will be quite high [1]. In the view of this, a purposeful change in the properties of the working fluid (in particular, the heat capacity) in the case of reagent or reagent-free exposure is of crucial importance.

The decrease in the heat capacity of water during the dissolution of various physical substances in it is clearly illustrated in the handbooks on the thermodynamic properties of solutions [2]. Based on this fact, at the end of the 70s of the 20th century, A. I. Kalina proposed a new thermodynamic cycle that involves the use of a mixture of ammonia and water as a working fluid. The advantages of such a combination are the exothermicity

This work is licensed under a Creative Commons Attribution 4.0 International License.

© Volodymyr H. Mykhailenko, Yevhen F. Lukianov, Olha I. Lukianova, Tamara S. Vitkovska, Oleksandr Ye. Khinievich, 2023